# Production of D-tagatose, bioethanol, and microbial protein from the dairy industry by-product whey powder using an integrated bioprocess

wei Ma[1], Fengyi Li[1], Longyue Li[1], Bin Li[2], Kangle Niu[1], Qinghua Liu[2], Laichuang Han[3], Lijuan Han[1], and Xu Fang[1]

[1]Shandong University
[2]Shandong Henglu Biotechnology Co., Ltd.
[3]Jiangnan University

August 17, 2023

**Abstract**

We designed and constructed a green, sustainable, and nongenetically modified organism (non-GMO) bioprocess to efficiently coproduce D-tagatose, bioethanol, and microbial protein from whey powder. First, a one-pot biosynthesis process involving lactose hydrolysis and D-galactose redox reactions for D-tagatose production was established in vitro via a three-enzyme cascade. Second, a nicotinamide adenine dinucleotide phosphate-dependent galactitol dehydrogenase mutant, D36A/I37R, based on the nicotinamide adenine dinucleotide-dependent polyol dehydrogenase from Paracoccus denitrificans was created through rational design and screening. Moreover, an NADPH recycling module was created in the oxidoreductive pathway, and the tagatose yield increased by 3.35-fold compared with that achieved through the pathway without the cofactor cycle. The reaction process was accelerated using an enzyme assembly with a glycine–serine linker, and the tagatose production rate was 9.28-fold higher than the initial yield. Finally, Saccharomyces cerevisiae was introduced into the reaction solution, and 266.5 g of D-tagatose, 371.3 g of bioethanol, and 215.4 g of dry yeast (including 38% protein) were obtained from 1 kg of whey powder (including 810 g lactose). This study provides a promising non-GMO process for functional food (D-tagatose) production. Moreover, this process fully utilized whey powder, demonstrating good atom economy.

Production ofD-tagatose, bioethanol, and microbial protein from the dairy industry by-product whey powder using an integrated bioprocess

Wei Ma [1], Fengyi Li [1], Longyue Li [1] Bin Li[2], Kangle Niu [1], Qinghua Liu[2], Laichuang Han [3], Lijuan Han[1]* and Xu Fang [1, 4] *

1. State Key Laboratory of Microbial Technology, Shandong University, Qingdao, Shandong, 266237, China

2. Shandong Henglu Biotechnology Co., Ltd., Jinan, Shandong, 250013, China

3. School of Biotechnology, Jiangnan University, Wuxi, Jiangsu, 214122, China

4. Rongcheng Huihai Chuangda Biotechnology Co., Ltd., Weihai, Shandong 264300, China

***** Correspondence:

Xu Fang, E-mail:*fangxu@sdu.edu.cn*,*Tel:(+86)*-532-5863-1507;

Lijuan Han, E-mail:*201820286@mail.sdu.edu.cn*,*Tel:* 17860821513.

**Keywords:** D-tagatose, oxidoreductive pathway, whey powder, cofactor balance, NADPH cycling, computer-aided screening

**Abbreviations**

GDH, galactitol dehydrogenase; GRAS, generally recognized as safe; GS-linker, glycine–serine linker; IPTG, isopropyl-beta-D-thiogalactopyranoside; NAD(H), nicotinamide adenine dinucleotide; NADP(H), nicotinamide adenine dinucleotide phosphate; non-GMO, nongenetically modified organism; *Pd* PDH, polyol dehydrogenase from *Paracoccus denitrificans* ; WP, whey powder; XR, aldose reductase.

**Abstract:**

We designed and constructed a green, sustainable, and nongenetically modified organism (non-GMO) bioprocess to efficiently coproduceD-tagatose, bioethanol, and microbial protein from whey powder. First, a one-pot biosynthesis process involving lactose hydrolysis and D-galactose redox reactions forD-tagatose production was established *in vitro*via a three-enzyme cascade. Second, a nicotinamide adenine dinucleotide phosphate-dependent galactitol dehydrogenase mutant, D36A/I37R, based on the nicotinamide adenine dinucleotide-dependent polyol dehydrogenase from *Paracoccus denitrificans* was created through rational design and screening. Moreover, an NADPH recycling module was created in the oxidoreductive pathway, and the tagatose yield increased by 3.35-fold compared with that achieved through the pathway without the cofactor cycle. The reaction process was accelerated using an enzyme assembly with a glycine–serine linker, and the tagatose production rate was 9.28-fold higher than the initial yield. Finally, *Saccharomyces cerevisiae*was introduced into the reaction solution, and 266.5 g ofD-tagatose, 371.3 g of bioethanol, and 215.4 g of dry yeast (including 38% protein) were obtained from 1 kg of whey powder (including 810 g lactose). This study provides a promising non-GMO process for functional food (D-tagatose) production. Moreover, this process fully utilized whey powder, demonstrating good atom economy.

## 1. Introduction

D-tagatose is widely used in the food and pharmaceutical industry and is receiving increasing attention for its disease-modifying properties in controlling diabetes and obesity, as a blood metabolism regulator, and for its health-promoting effects.[1–3] D-tagatose is an ideal substitute for sucrose owing to its high sweetness and low calorific value (92% as sweet and 30% of the energy of an equivalent amount of sucrose).[3] It is an epimer ofD-fructose and a ketose isomer ofD-galactose that is classified as a "rare sugar" because of its limited occurrence in nature.[1]

D-tagatose can be chemically synthesized using calcium catalysts and strong acids. The process is energy-intensive and requires complex purification steps.[1,4]Therefore, environmentally friendly biosynthesis technology for producing tagatose should be developed. D-tagatose has been produced using L-arabinose isomerase *in vitro* .[5–7] However, the theoretical conversion rate of the isomerase reaction is less than 0.5 mol/mol galactose at room temperature because of the unfavorable thermodynamic equilibrium ($\Delta\Gamma^{\circ} = 4.96$ kJ $mol^{-1}$ at 298.15 K).[8,9]

Recently, Sha et al. reported that the conversion rate of tagatose from galactitol reached 91% through oxidation.[10] Liu et al. constructed an oxidoreductive reaction with aldose reductase (XR) and galactitol dehydrogenase (GDH) in *Saccharomyces cerevisiae*for producing tagatose from lactose.[11] The theoretical conversion rate of the oxidoreductive pathway is higher than that of the isomerase reaction because of the lack of a reverse reaction in the oxidoreductive pathway for tagatose production. However, XR and GDH exhibit coenzyme dependence on $NADP^+$ and $NAD^+$, respectively; this difference in the coenzyme dependence of XR and GDH limited the target production yield.

Moreover, improving the economics of the production process in industrial production is important. Many scientists are looking for cheap materials as an alternative to galactose or galactitol. Whey, a by-product of the dairy industry, is abundant and inexpensive. Global production is estimated to be approximately 160 million tons per year.[12] Whey is an ideal substrate forD-tagatose production because it is lactose-rich. Simultaneously, whey contains proteins, fats, trace elements, and other nutrients that facilitate microbial

fermentation. Thus, an efficient bioprocess should be developed to produce D-tagatose and utilize the nutrients in whey powder (WP).

Herein, D-tagatose was synthesized using lactose from WP through oxidoreductive pathways. Subsequently, the coenzyme dependence of polyol dehydrogenase from *Paracoccus denitrificans*(*Pd* PDH) in the oxidoreductive pathways was modified from $NAD^+$ to $NADP^+$ using rational design for improving the tagatose yield. Moreover, the reaction process was accelerated using an enzyme assembly with a glycine–serine linker (GS-linker). Furthermore, the efficient coproduction ofD-tagatose, bioethanol, and microbial protein from WP was achieved. This study provides a promising application forD-tagatose biosynthesis while improving the economics of WP processing.

## 2. Materials and methods

### 2.1 Chemicals, plasmids, and culture media

Lactose, galactitol, NADH, NADPH, $NAD^+$, and $NADP^+$ were purchased from Coolaber Co. Ltd. (Beijing, China). The five types of WP were obtained from Qianwei Biotech (Shanghai, China), Miaolingziwei Biotech (Henan, China), Wanbang Biotech (Henan, China), Gushuo Biotech (Henan, China), and Fengtai Biotech (Shandong, China). The $\beta$ -galactosidase with ˜$1.2 \times 10^5$ U was purchased from Weilan Biotech (Shandong, China). The KOD-Plus-Mutagenesis Kit was purchased from Toyobo Co., Ltd. (Osaka, Japan). ABclonal MultiF Seamless Assembly was purchased from ABclonal Technology Co., Ltd. (Wuhan, China). pET-32a was purchased from Invitrogen (Carlsbad, CA, USA). Ampicillin and isopropyl-beta-D-thiogalactopyranoside (IPTG) were purchased from Gen-View Scientific Inc. (El Monte, CA, USA).*Escherichia coli* DH5α and *E. coli* BL21 (DE3) were purchased from Tsingke Biotechnology Co., Ltd. and TransGen Biotech (Beijing, China), respectively. Primers were synthesized by Ruibiotech Co., Ltd. (Beijing, China). Phanta®Max Super-Fidelity DNA Polymerase was purchased from Vazyme Biotech Co., Ltd. (Nanjing, China). Any other chemicals used in this study were analytical grade and obtained commercially unless otherwise noted.

### 2.2 Genetic constructs and site-directed mutagenesis

The gene coding for *Ps* XR (GenBank ID: XP_001385181) was amplified from the genome of *Pichia stipites.* Genes coding for*Pd* PDH from *Paracoccus denitrificans* (GenBank ID: WP_011751060), *Rl* GDH from *Rhizobium leguminosarum*(GenBank ID: WP_011650422.1), EutM from *Salmonella enterica*(GenBank ID: NP_461400.1), and fbaB (SpyTag-Catcher) from*Streptococcus pyogenes* (GenBank ID: NZ_LS483338.1) were synthesized by BGI Genomics Co., Ltd. (Shenzhen, China). All the above genes were amplified with primers harboring a homologous arm and ligated into pET-32a to obtain the recombinant vectors pET-32a-*Ps* XR, pET-32a-*Pd* PDH, pET-32a-*Rl* GDH, and pET-32a-EutM. All mutants were constructed using pET-32a-*Pd* PDH as a template for the KOD-Plus-Mutagenesis Kit. Strains and plasmids used in this study are listed in Table S1, and primers are summarized in Table S2.

### 2.3 Expression and purification

Recombinant plasmids, including pET-32a-*Ps* XR, pET-32a-*Rl* GDH, pET-32a-*Pd* PDH, and mutant *Pd* PDH, were transformed into *E. coli* BL21 (DE3) cells. Recombinant strains were precultured in 20-mL LB media with 10 μg $mL^{-1}$ ampicillin at 37 °C and 220 rpm for 24 h. Subsequently, a 20-mL preculture was inoculated into 1-L LB medium (with 10 μg $mL^{-1}$ ampicillin) at 37 °C and 200 rpm until the optical density at 600 nm reached 0.6–0.8. Then, 0.1 M IPTG was added, and incubation continued at 16 °C with shaking at 180 rpm for 20 h for enzyme expression. Sodium dodecyl-sulfate polyacrylamide gel electrophoresis analysis and His-tagged protein purification were performed as previously described.[13]

### 2.4 Activity assays and kinetic parameters

The activity was assayed by measuring the reduction of NAD(P) or the oxidation of NAD(P)H at 340 nm (e = 6.22 $mM^{-1}cm^{-1}$) at 30 °C using a spectrophotometer (AMR-100 Microplate Reader, Hangzhou, China).[10] The standard assay mixture for *Ps* XR contained 50 mM galactose in 100 mM Tris-HCl (pH 8.0) buffer. The standard assay mixture for*Rl* GDH, *Pd* PDH, and its mutants contained 50 mM galactitol in 100 mM

Tris-HCl (pH 8.0) buffer. Reactions were started by adding 0.25 mL of a 10 mM NAD(P) or NADPH solution to a final volume of 1.0 mL. One unit is a protein that produces or consumes 1 μM of NADH/NADPH per second. The $K_m$ and $k_{cat}$values were calculated using the Michaelis–Menten equation by nonlinear fitting using GraphPad Prism 9. The results are showed in Table 1 and Table 2.

### 2.5 Hydrolysis enzymatic synthesis and fermentation

Enzyme reactions were performed based on the conditions in Table 3. Furthermore, reaction conditions were investigated, including temperature, pH value, buffer type, concentration, and the *Ps* XR and *Pd* $PDH^{D36A/I37R}$ ratio, as shown in Figure S1. WP was hydrolyzed in citrate buffer at pH 5.5, 55 °C with a suitable amount of $\beta$ -galactosidase. Enzymatic hydrolysis was performed in a conical flask containing 122 g/L WP or 100 g/L lactose, 50 mM citrate buffer (pH 5.5, 55 °C), and a suitable amount of $\beta$ -galactosidase for 3 h. Enzymatic synthesis and fermentation were performed in a conical flask containing previously obtained enzymatic hydrolysates, 100 mM Tris-HCl buffer (pH 8.0, 30 °C), suitable amounts of*Pd* PDH-*Ps* XR complex, cofactor NADPH, and yeast cells with a final $A_{600}$ = 1. For the fermentation of enzymatic hydrolysates derived from lactose, 2% tryptone was required. The protein content of the WP solution and yeast cells was determined using a BCA Protein Assay Kit, as previously reported.[14]

### 2.6 Analytical methods

The reaction was stopped by placing it in a boiling bath, and the reaction solution was centrifuged at 16,200 × *g* for 2 min, and the supernatant was filtered with a 0.22-μm organic phase membrane. The concentrations of galactose, galactitol, ethanol, and tagatose were determined using high-performance liquid chromatography equipped with a refractive index detector (RI detector L2490, HITACHI, Japan) using a Shodex SP-0810 column (300 × 8 mm, Showa Denko K.K., Tokyo, Japan). The mobile phase was double distilled water, and the samples were separated at 70 °C at a flow rate of 1 mL $min^{-1}$. The retention times of galactose, galactitol, and tagatose were 9.91, 21.83, and 14.29 min, respectively. The formation of scaffolds was confirmed by negative stain transmission electron microscopy, as previously described.[15]

### 2.7 Interaction analysis and substrate docking

The docking results and interaction analysis were shown using LigPlot software. The docking between *Pd* PDH (PDBID: 7E6O) and the cofactors $NADP^+$ (PubChem CID: 5886) and $NAD^+$ (PubChem CID: 5892) was performed using the Schrodinger Suites 2021-4.

## 3. Results

### 3.1 Designing the oxidoreductive pathways for$_D$-tagatose production

We constructed the oxidoreductive pathways for producing tagatose from lactose. The synthesis pathway was composed of three modules, as shown in Figure 1: (1) lactose hydrolysis module (with$\beta$ -galactosidase); (2) galactose reduction module (with aldose reductase, EC: 1.1.1.307); and (3) galactitol oxidation module (with galactitol dehydrogenase, EC: 1.1.1.14). A three-enzyme cascade converting lactose into tagatose (Pathway I) was designed using$\beta$ -galactosidase, NADPH-preferring *Ps* XR from *P. stipites* (GenBank ID: XP_001385181), $NAD^+$-dependent*Pd* PDH from *P. denitrificans* (GenBank ID: WP_011751060), or the $NAD^+$-dependent *Rl* GDH from *R. leguminosarum* (GenBank ID: WP_011650422.1) (Figure 1A). The coenzyme dependence of *Ps* XR and *Rl* GDH or *Pd* PDH is different. Furthermore, we designed a novel Pathway II for constructing a cofactor cycle between the reduction and oxidation modules (Figure 1B).

### 3.2 Constructing the NADPH cycle with the modification of*Pd*PDH

There is no $NADP^+$-dependent galactitol dehydrogenase in the ENZYME database, and it is difficult to mine the $NADP^+$-dependent galactitol dehydrogenase in nature. Therefore, we must develop a rational design for $NADP^+$-dependent galactitol dehydrogenase. We mined*Pd* PDH and *Rl* GDH from the enzyme bank, and their dehydrogenase activities were compared (Figure S2A). The activity of*Pd* PDH with respect to galactitol

dehydrogenation was 17.29 times greater than that of *Rl* GDH (25.42 and 1.47 U $mg^{-1}$, respectively) (Figure S2B). Therefore,*Pd* PDH was selected as the template for the rational design.

We docked *Pd* PDH (PDBID: 7E6O) with the cofactor $NAD^+$ (PubChem CID: 5892) using the Schrodinger software, and the docking results are shown using LigPlot software (Figure S3A). We selected 22 amino acids within 5 Å of $NAD^+$ that interact with the cofactor based on hydrogen bond or hydrophobic interaction. The *Pd* PDH-$NAD^+$combination model was predicted using the CSR-SALAD website (Table S3 and Table S4). According to the predicted results, we designed 100 mutants of *Pd* PDH (Table S5) based on 13 amino acid residues (Figure S3B). Subsequently, a point mutation of *Pd* PDH was simulated using Schrodinger software, and the mutants were docked with the cofactor $NADP^+$. Then, the docking binding energies of the mutants were counted (Table S5). A total of 14 mutants were selected according to their lower binding energies, indicating that they had a higher affinity for $NADP^+$ than the other mutants. Furthermore, their specific activities for $NAD^+$ and $NADP^+$ were measured. As shown in Table 1, nine mutants completely reversed the cofactor preference and exhibited improved specific activity toward $NADP^+$. Six mutants had $NADP^+$ activities of more than 15 U $mg^{-1}$; particularly, the $NADP^+$activity of the D36A/I37R mutant reached 19.4 U $mg^{-1}$. However, the triple mutants (A14T/D36A/I37R and A14S/D36A/I37R) did not improve their activities further than those of the double mutants. The single mutants (D36A, D36G, and I37R) exhibited no activity against $NADP^+$. The screening accuracy was increased sevenfold the computer-aided screening (9/14) compared with the original screening (9/100).

The kinetic parameters of *Pd* PDH mutants and the wild-type are shown in Table 2. The$K_m$ value of $NADP^+$ with the D36A/I37R mutant was 0.942 mM and was lower than that of the wild-type enzyme (infinite), proving that there was a substantial increase in the affinity of the D36A/I37R mutant for $NADP^+$. Moreover, the specificity constant ($k_{cat}/K_m$ ) of the D36A/I37R mutant toward $NADP^+$ reached 0.322 $mM^{-1}s^{-1}$, whereas that of the wild-type was 0 $mM^{-1}s^{-1}$. Conversely, the specificity constant ($k_{cat}/K_m$ ) of the wild-type toward $NAD^+$ was 0.4872 $mM^{-1}s^{-1}$, whereas that of the D36A/I37R mutant was 0 $mM^{-1}s^{-1}$. Furthermore, we identified the binding free energy of each cofactor with the wild-type and its mutant D36A/I37R (Table S6). The binding free energy of the D36A/I37R mutant toward $NADP^+$ decreased by 54% (from -8.011 to -12.335 kcal $mol^{-1}$), whereas that toward $NAD^+$ increased by 46% (from -13.614 to -7.325 kcal $mol^{-1}$). These results suggested that the binding affinity of the D36A/I37R mutant toward $NADP^+$ was higher than that toward $NAD^+$. Therefore, we obtained an $NADP^+$-dependent*Pd* $PDH^{D36A/I37R}$ for performing the NADPH cycle during tagatose production.

### 3.3 Producing the tagatose with various conditions

The lactose from WP was completely hydrolyzed into galactose and glucose with $\beta$ -galactosidase (Table S7). The tagatose production through Pathways I or II using *Ps* XR and *Pd* PDH or the mutant*Pd* $PDH^{D36A/I37R}$ was performed under various conditions. $_D$-tagatose was not produced under Pathway I–Condition 1 (Figure 2A and Table 3), although 3.7 mM galactitol was produced after 48 h. We speculated that galactose was converted into galactitol by *Ps* XR; however, no tagatose was produced from galactitol with wild-type *Pd* PDH without $NAD^+$. Under Pathway I–Condition 2 and Pathway II–Condition 1, 1.46 mM and 6.30 mM tagatose was produced after 96 h (Figures 2B–C), with a conversion rate of 0.07 and 0.31 mol/mol lactose, respectively, though the galactitol yields were similar. The tagatose yield of Pathway II–Condition 1 was 4.35-fold higher than that of Pathway I–Condition 2. This result proved that tagatose production was considerably improved with the cofactor cycle module.

The enzyme assembly strategies were applied to improve the tagatose yield. First, a fused protein was prepared with the GS-linker between*Ps* XR and *Pd* $PDH^{D36A/I37R}$ (Figure 3A, Pathway II–Condition 3; Figures S4A and B). Subsequently, we designed the SpyTag003/Catcher003 connection system between *Ps* XR and*Pd* $PDH^{D36A/I37R}$ (Figure 3A: Pathway II–Condition 4/5; Figures S4A and B). Finally, the EutM-*Ps* XR-*Pd* $PDH^{D36A/I37R}$-system was constructed using EutM-SpyCatcher003, SpyTag003-*Ps* XR, and SpyTag003-*Pd* $PDH^{D36A/I37R}$ (Figure 3A: Pathway II–Condition 6; Figures S4C and D). The*Pd* $PDH^{D36A/I37R}$ activities did not considerably change after ligation of SpyTag003 or SpyCatcher003 in the N-terminus or C-terminus. However, ligation into the C-terminus (Figure S4E) impaired the activity of *Ps* XR, whereas the ligation in

the N-terminus did not change its activity (Figure S4F). Therefore, we selected the ligation of SpyTag003 or SpyCatcher003 in the N-terminus or C-terminus with *Pd* $PDH^{D36A/I37R}$ and in the N-terminus with*Ps* XR.

The tagatose yield with the GS-linker strategy (Pathway II–Condition 3) was the highest among these cascade enzyme reactions (Figure 3B) and was 1.79-fold higher compared with that of the free enzyme system (Pathway II–Condition 2) at 24 h. The tagatose yield with the N-SpyTag003-*Pd* $PDH^{D36A/I37R}$ and N-SpyCatcher003-*Ps* XR systems (Pathway II–Condition 4) increased by 19% at 24 h compared with that of the free enzyme system. The activities of the C-SpyTag003-*Pd* $PDH^{D36A/I37R}$and N-SpyCatcher003-*Ps* XR systems (Pathway II–Condition 5) did not considerably change compared with that of the free enzyme system, and the activity of the EutM-scaffold system (Pathway II–Condition 6) was not higher than that of the free enzyme system.

Finally, the production of tagatose was improved using a fed-batch culture strategy comprising *Pd* $PDH^{D36A/I37R}$ per 12 h based on Pathway II–Condition 3. This produced 14.5 mM tagatose after 96 h with a conversion rate of 0.72 mol/mol lactose, an increase of 9.28-fold compared with Pathway I–Condition 2.

### 3.4 Coproduction of $_{D}$-tagatose, bioethanol, and microbial protein from WP

WP is a by-product of the dairy industry during the cheese production process. We analyzed the chemical composition of five different commercial sources of WP and found that the lactose content was 70%–80%, and the soluble protein content was 0.2%–0.7% (Table S8).$\beta$ -Galactosidase hydrolyzed lactose into glucose and galactose. Galactose is used to synthesize tagatose, while glucose and other nutrients can be used for yeast growth and ethanol production. Therefore, a scheme workflow was designed to illustrate the process for producing tagatose, bioethanol, and microbial protein from WP (Figure 4).

The WP solution contained 100-g/L lactose, which was hydrolyzed by$\beta$ -galactosidase to yield 52.4-g/L glucose and galactose. Then, galactose in the enzymatic hydrolysate was converted into 32.9 g/L tagatose based on Pathway II–condition 3 (Figure 5A, Table 4); however, the glucose in the enzymatic hydrolysate was not consumed. Subsequently, 0.8 g *S. cerevisiae* was added into the enzymatic hydrolysate, and the glucose was entirely consumed in 12 h, whereas there was no obvious change in $_{D}$-tagatose concentration (Figure 5B). First, the yeast cell was separated using solid/liquid separation, and 26.6 g/L yeast cells (dry weight, including 38% protein) was obtained. Second, the ethanol was distilled from the broth using reduced pressure distillation, and 45.8 g/L ethanol under anaerobic conditions was produced. Third, tagatose was purified through concentration and crystallization.

## 4. Discussion

The conversion between aldose and ketose forms of sugars can be catalyzed by isomerase in one step or by oxidoreductase in two steps. Until 2018, many studies had focused on the isomerase reaction using$_{L}$-arabinose isomerase to produce tagatose from galactose. Several studies attempted to increase the conversion rate using immobilized enzymes,[16] recombinant cell expression,[17-20] immobilized recombinant cells,[8,21] cell encapsulation,[22] or cell surface display.[23,24] However, the isomerase reaction had a lower conversion rate because of the unfavorable thermodynamic equilibria.[8,9] Therefore, an oxidoreductive pathway was selected for tagatose synthesis in this study.

Oxidoreductases are usually cofactor-dependent, and the imbalance of cofactors in the cascade reaction may limit the conversion of the substrate. Alleviating the redox imbalance has been reported to be beneficial for improving the yield of the target production using cofactor engineering strategies.[25-28] Cahn et al. developed a general tool named CSR-SALAD to help reverse the cofactor preference of oxidoreductases due to the large demand for balancing cofactor availability.[27] Cofactor reversal has now been realized and applied to many enzymes.[29,30] For example, alcohol dehydrogenase in *Clostridium autoethanogenum* was modified to NADH dependence, resulting in improved growth and ethanol production.[31] Xylitol dehydrogenase was modified to be NADPH-dependent to reduce cofactor imbalance in xylose assimilation, and the engineered *S. cerevisiae* exhibited high xylose utilization and ethanol production capabilities.[13,32-33] To alleviate the

cofactor imbalance in the biosynthesis of branched-chain amino acids, the coenzyme preference of ketol-acid reductoisomerase was altered from NADPH to NADH.[34,35] However, cofactor engineering in the redox pathway of tagatose synthesis has not yet been reported. Therefore, we designed and demonstrated the oxidoreductive Pathway II and the conversion rate was greatly improved (Figure 3).

Basic amino acid residues in the cofactor binding region are believed to favor the binding of NADPH, whereas acidic amino acids facilitate the affinity of NADH.[36,37] Based on this principle, we designed 100 mutants of *Pd* PDH (Table S5). Complete reversal of the coenzyme specificity was achieved with those containing D36A(G/R/H/K/I/F)/I37R (Table 2), which agrees with the results of a previous study.[13] We investigated the binding mechanism between the mutants or the wild-type *Pd* PDH and the $NAD^+$ or $NADP^+$ cofactors. Interactions between protein and ligand, such as strong hydrogen interactions, are essential for stable binding, and steric hindrance and electrostatic repulsion may hinder their affinity.[38,39] In the wild-type *Pd* PDH, the adenosine portion of $NAD^+$ could be stabilized by strong hydrogen interactions between the 2'-and 3'-hydroxyl groups and the negatively charged amino acid Asp36, as shown in Figure S5A. In the D36A/I37R mutant, the 2'-and 3'-hydroxyl groups of $NAD^+$ were pushed apart by the amino group of Arg37 due to spatial site resistance and electrostatic repulsion, and strong hydrogen interaction was lacking between the 2'- and 3'-hydroxyl groups of $NAD^+$ and Ala36, resulting in less interaction with D36A/I37R than that in the wild-type *Pd* PDH. For the $NADP^+$ cofactor, mutation of the Ile37 side chain to Arg37 resulted in a stable and strong hydrogen interaction with the 2'-phosphate group of $NADP^{+,}$ as shown in Figure S5. Therefore, the $K_m$ values of $NAD^+$ and $NADP^+$ of *Pd* PDH were 0.7 mM and infinity, respectively, whereas those of the*Pd* $PDH^{D36A/I37R}$ were infinity and 0.942 mM, respectively.

Enzyme assembly could improve the efficiency of the reaction. Various strategies for constructing artificial multienzyme complexes have been widely reported and successfully applied, including fusion protein technology with a linker,[40,41]SpyTag003/SpyCatcher003,[42] and self-assembling scaffold-EutM.[43] We constructed the GS-linker (Figure S4B), SpyTag003/SpyCatcher003 (Figures S4A and B), and EutM-scaffold systems (Figures S4C and D) and found that the GS-linker system played the best-facilitating role. We speculated that this linkage maintained a suitable distance between *Ps* XR and*Pd* $PDH^{D36A/I37R}$, allowing a faster reaction transfer. The SpyTag003/Catcher003 linkage system may form a longer distance compared with that of the GS-linker system because the SpyTag003 and SpyCatcher003 were all fused to the N-terminus or C-terminus of the protein with the same GS-linker (Figure 3A). Therefore, the tagatose yield only increased by 19% at 24 h compared with that of the free enzyme system. With the EutM-scaffold system, we speculated that this linkage may not have brought the enzymes spatially closer together as the activity was not considerably improved compared with that of the free enzyme system.

The reuse of industrial waste is important for saving energy and reducing emissions, while the conversion of waste into high-value products is an important method for establishing a sustainable bioeconomy. Whey, a by-product of the dairy industry, is an environmental pollutant.[12] However, whey has lactose and abundant nitrogen sources. Thus, whey is a suitable material for microbial fermentation. Engineered *E. coli* strain was used to produce tagatose from cheese whey.[18,28] However, nongenetically modified organism (non-GMO) tagatose production technology is being explored to obtain an increased tagatose yield from lactose. Herein, we demonstrated an enzyme cascade pathway for producing$_D$-tagatose from 1 kg of WP, including 81% lactose, and the tagatose yield from lactose and WP reached 0.32 and 0.27 g/g, respectively. In this reaction, we found that galactose was entirely consumed; by contrast, there was no change in glucose concentration (Figure 5). These conversion efficiencies are similar to those of microbial cell factories.[11,28] However, this study constructed a more robust non-GMO technology, which avoids consumer anxiety about genetically modified technology. Furthermore, yeast fermentation in the enzyme reaction solution was performed without tagatose separation. We compared the ethanol production with and without adding nitrogen source after tagatose production, and no significant change in ethanol yields was observed (Figure 5). This suggested the presence of an abundant nitrogen source and trace elements in whey for yeast growth and ethanol production under anaerobic conditions. Moreover, no change in tagatose concentration in the broth was observed, suggesting that natural *S. cerevisiae* cannot utilize tagatose. Finally, we obtained 371.3 g of ethanol and 215.4 g of dry yeast cells from 1 kg of WP, and the protein content in the dry yeast was

approximately 38% (w/w) (Table S9). Bioethanol is an important fuel for mitigating global warming and conserving fossil fuels.[43]Microbial protein, or single-cell protein, has been regarded as an important protein reservoir for future nutritional needs.[44] Microbial proteins have been used as a feed or feed supplement.[45] Microbial proteins have good environmental benefits as an alternative to ruminant meat.[46] *S. cerevisiae* is considered a generally recognized as safe (GRAS) strain and is therefore a good candidate for microbial protein.[14,47,48]

## 5. Conclusion

Herein, we successfully created the $NADP^+$-dependent*Pd* $PDH^{D36A/I37R}$ and constructed the NADPH recycling module. By employing the constructed GS-linker system *in vitro* to assemble the oxidoreductases, the $_D$-tagatose yield from lactose (0.378 g/g) was 9.28-fold higher than the initial yield. Furthermore, whey, a by-product in cheese production, was used as the sole material for producing $_D$-tagatose, bioethanol, and microbial protein with an integrated bioprocess combined with enzyme cascade and anaerobic fermentation. Finally, 266.5 $g_D$-tagatose, 371.3 g bioethanol, and 215.5 g dry yeast (including 38% protein) were obtained from 1 kg WP (including 810 g lactose). The economic feasibility was improved owing to the expensive price of $_D$-tagatose, compared with those of bioethanol and microbial protein. Moreover, the risk of food safety was avoided owing to non-GMO technology. This bioprocess in which the dairy waste was entirely utilized helps reduce the net emission of carbon dioxide and drives sustainable development.

Acknowledgements

The authors would like to thank Dr. Sen Wang from State Key Laboratory of Microbial Technology of Shandong University for help and guidance in transmission electron microscopy. This work was supported by National Key R&D Program of China (No. 2018YFA0901700), National Natural Science Foundation of China (No. 32271526).

## Declaration of Competing Interest

The authors declare that they have no known competing financial interests or personal relationships that could have appeared to influence the work reported in this paper.

## Author Contributions

All authors contributed to the background research and writing of the article, as well as the editing. In addition, all authors have read and approved the final version of this manuscript.

## Research Data Policy

The original/source data and resources are available from the correspondence author Xu Fang (fangxu@sdu.edu.cn) on request.

## Chemical compounds studied in this article

$NAD^+$ (PubChem CID: 5892); $NADP^+$(PubChem CID: 5886); $_D$-tagatose (PubChem CID:439312);$_D$-Galactose (PubChem CID:6036); Galactitol (PubChem CID:11850).

## References

[1] Roy, S.; Chikkerur, J.; Roy, S. C.; Dhali, A.; Kolte, A. P.; Sridhar, M.; Samanta, A. K. Tagatose as a potential nutraceutical: Production, properties, biological roles, and applications. *J Food Sci.* **2018** , *83* (11), 2699-2709. https://doi.org/10.1111/1750-3841.14358

[2] Buemann, B.; Toubro, S.; Raben, A.; Blundell, J.; Astrup, A. The acute effect of $_D$-tagatose on food intake in human subjects. *Br. J. Nutr.* **2007** . *84* (2), 227-231. https://doi.org/10.1017/S000711450000146X

[3] Guerrero-Wyss, M.; Duran Aguero, S.; Angarita Davila, L.$_D$-tagatose is a promising sweetener to control glycaemia: a new functional food. *Biomed Res Int.* **2018** , 8718053. https://doi.org/10.1155/2018/8718053

[4] de Bruyn, C. A. L.; van Ekenstein, W. A. Action des alcalis sur les sucres. V: Transformation de la galactose. Les tagatoses, et la galtose. *Recueil des Travaux Chimiques des Pays-Bas et de la Belgique.* **1897** , *16* (9), 262-273. https://doi.org/10.1002/recl.18970160903

[5] Zhang, G.; An, Y.; Parvez, A.; Zabed, H. M.; Yun, J.; Qi, X. Exploring a highly $_{D}$-galactose specific$_{L}$-arabinose isomerase from *Bifidobacterium adolescentis* for $_{D}$-tagatose production. *Front Bioeng Biotechnol.* **2020** , *8* , 377. https://doi.org/10.3389/fbioe.2020.00377

[6] Zheng, Z.; Mei, W.; Xia, M.; He, Q.; Ouyang, J. Rational design of *Bacillus coagulans* NL01 $_{L}$-arabinose isomerase and use of its F279I variant in $_{D}$-tagatose production.*J. Agric. Food Chem.* **2017** , *65* (23), 4715-4721. https://doi.org/10.1021/acs.jafc.7b01709

[7] Jeong, D. W.; Hyeon, J. E.; Shin, S. K.; Han, S. O. Trienzymatic complex system for isomerization of agar-derived$_{D}$-galactose into $_{D}$-tagatose as a low-calorie sweetener. *J Agric Food Chem.* **2020** ,*68* (10), 3195-3202.*https://doi.org/10.1021/acs.jafc.9b07536*

[8] Hong, Y. H.; Lee, D. W.; Lee, S. J.; Choe, E. A.; Kim, S. B.; Lee, Y. H.; Cheigh, C. I.; Pyun, Y. R. Production of$_{D}$-tagatose at high temperatures using immobilized*Escherichia coli* cells expressing $_{L}$-arabinose isomerase from *Thermotoga neapolitana* . *Biotechnol Lett.***2007** *, 29* (4), 569-574.*https://doi.org/10.1007/s10529-006-9277-2*

[9] Kim, J. H.; Lim, B. C.; Yeom, S. J.; Kim, Y. S.; Kim, H. J.; Lee, J. K.; Lee, S. H.; Kim, S. W.; Oh, D. K. Differential selectivity of the *Escherichia coli* cell membrane shifts the equilibrium for the enzyme-catalyzed isomerization of galactose to tagatose. *Appl Environ Microbiol.* **2008** , *74* (8), 2307-2313.*https://doi.org/10.1128/AEM.02691-07*

[10] Sha, F.; Zheng, Y.; Chen, J.; Chen, K.; Cao, F.; Yan, M.; Ouyang, P. $_{D}$-tagatose manufacture through bio-oxidation of galactitol derived from waste xylose mother liquor. *Green Chem.* **2018** , *20* (10), 2382-2391.*https://doi.org/10.1039/C8GC00091C*

[11] Liu, J. J.; Zhang, G. C.; Kwak, S.; Oh, E. J.; Yun, E. J.; Chomvong, K.; Cate, J. H. D.; Jin, Y. S. Overcoming the thermodynamic equilibrium of an isomerization reaction through oxidoreductive reactions for biotransformation. *Nat Commun.* **2019** ,*10* (1), 1356. https://doi.org/10.1038/s41467-019-09288-6

[12] Ding, J.; S. You.; W. Ba.; H. Zhang.; H. Chang.; W. Qi.; R. Su.; Z. He. Bifunctional Utilization of Whey Powder as a Substrate and Inducer for Beta-Farnesene Production in an Engineered *Escherichia Coli* . *Bioresour Technol* . **2021** , *341,* 125739. https://doi.org/10.1016/j.biortech.2021.125739

[13] Watanabe, S.; Kodaki, T.; Makino, K. Complete reversal of coenzyme specificity of xylitol dehydrogenase and increase of thermostability by the introduction of structural zinc. *J Biol Chem.* **2005** , *280* (11), 10340-10349.*https://doi.org/10.1074/jbc.M409443200*

[14] Xu, X.; Zhang, W.; You, C.; Fan, C.; Ji, W.; Park, J. T.; Kwak, J.; Chen, H.; Zhang, Y. P. J.; Ma, Y. Biosynthesis of Artificial Starch and Microbial Protein from Agricultural Residue. *Sci. Bull.***2023,** *68* (2), 214-23. https://dx.doi.org/10.1016/j.scib.2023.01.006.

[15] Zhang, G.; Quin, M. B.; Schmidt-Dannert, C. Self-assembling protein scaffold system for easy *in vitro* coimmobilization of biocatalytic cascade enzymes. *ACS Catalysis,* **2018** ,*8* (6), 5611-5620.*https://doi.org/10.1021/acscatal.8b00986*

[16] Bortone, N.; Fidaleo, M. Immobilization of the recombinant (His)6-tagged$_{L}$-arabinose isomerase from *Thermotoga maritima* on epoxy and cupper-chelate epoxy supports. *Food Bioprod. Process.***2015** , *95* , 155-162.*https://doi.org/10.1016/j.fbp.2015.05.002*

[17] Zheng, Z.; Xie, J.; Liu, P.; Li, X.; Ouyang, J. Elegant and efficient biotransformation for dual production of$_{D}$-tagatose and bioethanol from cheese whey powder.*J. Agric. Food Chem.* **2019** , *67* (3), 829-835.*https://doi.org/10.1021/acs.jafc.8b05150*

[18] Zhang, G.; Zabed, H. M.; An, Y.; Yun, J.; Huang, J.; Zhang, Y.; Li, X.; Wang, J.; Ravikumar, Y.; Qi, X. Biocatalytic conversion of a lactose-rich dairy waste into $_{D}$-tagatose,$_{D}$-arabitol and galactitol using sequential whole cell and fermentation technologies. *Bioresour Technol.* **2022** ,*358* , 127422.*https://doi.org/10.1016/j.biortech.2022.127422*

[19] Jayamuthunagai, J.; Srisowmeya, G.; Chakravarthy, M.; Gautam, P. $_{D}$-tagatose production by permeabilized and immobilized *Lactobacillus plantarum* using whey permeate.*Bioresour Technol.* **2017** *, 235* , 250-255.*https://doi.org/10.1016/j.biortech.2017.03.123*

[20] Zhang, G.; Zabed, H. M.; Yun, J.; Yuan, J.; Zhang, Y.; Wang, Y.; Qi, X. Two-stage biosynthesis of $_{D}$-tagatose from milk whey powder by an engineered *Escherichia coli* strain expressing $_{L}$-arabinose isomerase from*Lactobacillus plantarum* . *Bioresour Technol.* **2020** ,*305* , 123010.*https://doi.org/10.1016/j.biortech.2020.123010*

[21] Xu, Z.; Li, S.; Fu, F.; Li, G.; Feng, X.; Xu, H.; Ouyang, P. Production of $_{D}$-tagatose, a functional sweetener, utilizing alginate immobilized *Lactobacillus fermentum* CGMCC2921 cells. *Appl Biochem Biotechnol.* **2012** , *166* (4), 961-973.*https://doi.org/10.1007/s12010-011-9484-8*

[22] Bober, J. R.; Nair, N. U. Galactose to tagatose isomerization at moderate temperatures with high conversion and productivity.*Nat Commun.* **2019** , *10* (1), 4548.*https://doi.org/10.1038/s41467-019-12497-8*

[23] Liu, Y.; Li, S.; Xu, H.; Wu, L.; Xu, Z.; Liu, J.; Feng, X. Efficient production of $_{D}$-tagatose using a food-grade surface display system. *J. Agric. Food Chem.* **2014** ,*62* (28), 6756-6762.*https://doi.org/10.1021/jf501937j*

[24] Guo, Q.; An, Y.; Yun, J.; Yang, M.; Magocha, T. A.; Zhu, J.; Xue, Y.; Qi, Y.; Hossain, Z.; Sun, W.; & Qi, X. Enhanced$_{D}$-tagatose production by spore surface-displayed$_{L}$-arabinose isomerase from isolated *Lactobacillus brevis* PC16 and biotransformation. *Bioresour Technol.***2018** , *247* , 940-946.*https://doi.org/10.1016/j.biortech.2017.09.187*

[25] Liu, J.; Li, H.; Zhao, G.; Caiyin, Q.; Qiao, J. Redox cofactor engineering in industrial microorganisms: strategies, recent applications and future directions. *J Ind Microbiol Biotechnol.***2018** , *45* (5), 313-327.*https://doi.org/10.1007/s10295-018-2031-7*

[26] You, C.; Huang, R.; Wei, X.; Zhu, Z.; Zhang, Y. P. Protein engineering of oxidoreductases utilizing nicotinamide-based coenzymes, with applications in synthetic biology. *Synth Syst Biotechnol.***2017** , *2* (3), 208-218.*https://doi.org/10.1016/j.synbio.2017.09.002*

[27] Cahn, J. K.; Werlang, C. A.; Baumschlager, A.; Brinkmann-Chen, S.; Mayo, S. L.; Arnold, F. H. A general tool for engineering the NAD/NADP cofactor preference of oxidoreductases. *ACS Synth Biol* .**2017** , *6 (2)* , 326-333.*https://doi.org/10.1021/acssynbio.6b00188*

[28] Liu, W.; Zhang, Z.; Li, Y.; Zhu, L.; Jiang, L. Efficient production of $_{D}$-tagatose via DNA scaffold mediated oxidoreductases assembly in vivo from whey powder. *Food Res. Int.***2023** , *166* , 112637.*https://doi.org/10.1016/j.foodres.2023.112637*

[29] Solanki, K.; Abdallah, W.; Banta, S. Extreme makeover: Engineering the activity of a thermostable alcohol dehydrogenase (AdhD) from *Pyrococcus furiosus* . *Biotechnol J.* **2016** ,*11* (12), 1483-1497.*https://doi.org/10.1002/biot.201600152*

[30] Iorgu, A. I.; Hedison, T. M.; Hay, S.; Scrutton, N. S. Selectivity through discriminatory induced fit enables switching of NAD(P)H coenzyme specificity in Old Yellow Enzyme ene-reductases.*FEBS J.* **2019** *, 286* (16), 3117-3128.*https://doi.org/10.1111/febs.14862*

[31] Maddock, D. J.; Patrick, W. M.; Gerth, M. L. Substitutions at the cofactor phosphate-binding site of a clostridial alcohol dehydrogenase lead to unexpected changes in substrate specificity.*Protein Eng. Des. Sel.* **2015** , *28* (8), 251-258. https:// doi.org/10.1093/protein/gzv028

[32] Watanabe, S.; Saleh, A. A.; Pack, S. P.; Annaluru, N.; Kodaki, T.; Makino, K. Ethanol production from xylose by recombinant*Saccharomyces cerevisiae* expressing protein engineered $NADP^+$-dependent xylitol dehydrogenase. *J Biol Chem.* **2007** , *130* (3), 316-319.

[33] Matsushika, A.; Watanabe, S.; Kodaki, T.; Makino, K.; Inoue, H.; Murakami, K.; Takimura, O.; Sawayama, S. Expression of protein engineered $NADP^+$-dependent xylitol dehydrogenase increases ethanol production from xylose in recombinant*Saccharomyces cerevisiae* . *Appl Microbiol Biot.***2008** , *81* (2), 243-255. https://doi.org/10.1007/s00253-008-1649-1

[34] Bastian, S.; Liu, X.; Meyerowitz, J. T.; Snow, C. D.; Chen, M. M.; Arnold, F. H. Engineered ketol-acid reductoisomerase and alcohol dehydrogenase enable anaerobic 2-methylpropan-1-ol production at theoretical yield in *Escherichia coli* . *Metab Eng.***2011** , *13* (3), 345-352. https://doi.org/10.1016/j.ymben.2011.02.004

[35] Brinkmann-Chen, S.; Flock, T.; Cahn, J. K.; Snow, C. D.; Brustad, E. M.; McIntosh, J. A.; Meinhold, P.; Zhang, L.; Arnold, F. H. General approach to reversing ketol-acid reductoisomerase cofactor dependence from NADPH to NADH.*Proc Natl Acad Sci U S A.* **2013** , *110* (27), 10946-10951. https://doi.org/10.1073/pnas.1306073110

[36] Chanique, A. M.; Parra, L. P. Protein engineering for nicotinamide coenzyme specificity in oxidoreductases: Attempts and challenges. *Front Microbiol* . **2018** , *9* , 194. https://doi.org/10.3389/fmicb.2018.00194

[37] Petschacher, B.; Staunig, N.; Muller, M.; Schurmann, M.; Mink, D.; De Wildeman, S.; Gruber, K.; Glieder, A. Cofactor specificity engineering of streptococcus mutans NADH oxidase 2 for $NAD(P)^+$ regeneration in biocatalytic oxidations.*Comput Struct Biotechnol* . **2014** , *9* , e201402005. https://doi.org/10.5936/csbj.201402005

[38] You, Z.-N.; Chen, Q.; Shi, S.-C.; Zheng, M.-M.; Pan, J.; Qian, X.-L.; Li, C.-X.; Xu, J.-H. Switching cofactor dependence of 7β-hydroxysteroid dehydrogenase for cost-effective production of ursodeoxycholic acid. *ACS Catalysis.* **2018** , *9* (1), 466-473. https://www.x-mol.com/paperRedirect/919853

[39] Jiang, Y.; Shen, Y.; Gu, L.; Wang, Z.; Su, N.; Niu, K.; Guo, W.; Hou, S.; Bao, X.; Tian, C.; Fang, X. Identification and characterization of an efficient$_D$-xylose transporter in *Saccharomyces cerevisiae* .*J Agric Food Chem.* **2020** , *68* (9), 2702-2710. https://doi.org/10.1021/acs.jafc.9b07113

[40] Grawe, A.; Stein, V. Linker engineering in the context of synthetic protein switches and sensors. *Trends Biotechnol.***2021** , *39* (7), 731-744. https://doi.org/10.1016/j.tibtech.2020.11.007

[41] Guo, H.; Yang, Y.; Xue, F.; Zhang, H.; Huang, T.; Liu, W.; Liu, H.; Zhang, F.; Yang, M.; Liu, C.; Lu, H.; Zhang, Y.; Ma, L. Effect of flexible linker length on the activity of fusion protein 4-coumaroyl-CoA ligase::stilbene synthase. *Mol Biosyst.* **2017** , *13*(3), 598-606. https://doi.org/10.1039/C6MB00563B

[42] Keeble, A. H.; Turkki, P.; Stokes, S.; Khairil Anuar, I. N. A.; Rahikainen, R.; Hytonen, V. P.; Howarth, M. Approaching infinite affinity through engineering of peptide-protein interaction. *Proc Natl Acad Sci U S A.* **2019** , *116* (52), 26523-26533. https://doi.org/10.1073/pnas.1909653116

[43] Manigandan, S.; Praveenkumar, T. R.; Anderson, A.; Maryam, A.; Mahmoud, E. Benefits of pretreated water hyacinth for enhanced anaerobic digestion and biogas production. *International Journal of Thermofluids* . **2023** , *19* , 100369. https://dx.doi.org/10.1016/j.ijft.2023.100369.

[44] Ritala, A.; Hakkinen, S. T.; Toivari, M.; Wiebe, M. G. Single Cell Protein-State-of-the-Art, Industrial Landscape and Patents 2001-2016. *Front Microbiol.* **2017** , *8* , 2009. https://dx.doi.org/10.3389/fmicb.2017.02009.

[45] Tuse, D. Single-Cell Protein: Current Status and Future Prospects. *Crit Rev Food Sci.* **1984** , *19*(4), 273-325. https://dx.doi.org/10.1080/10408398409527379.

[46] Humpenoder, F.; Bodirsky, B. L.; Weindl, I.; Lotze-Campen, H.; Linder, T.; Popp, A. Projected environmental benefits of replacing beef with microbial protein. *Nature.* **2022** , *605* (7908), 90-96.

https://doi.org/10.1038/s41586-022-04629-w

[47] Ma, J.; Sun, Y.; Meng, D.; Zhou, Z.; Zhang, Y.; Yang, R. Yeast proteins: The novel and sustainable alternative protein in food applications. *Trends Food Sci Technol* . **2023** , *135* , 190-201. https://doi.org/10.1016/j.tifs.2023.04.003

[48] Xia, S.; Song, J.; Li, K.; Hao, T.; Ma, C.; Shen, S.; Jiang, X.; Xue, C.; Xue, Y. Yeast protein-based meat analogues: Konjac glucomannan induces the fibrous structure formation by modifying protein structure. *Food Hydrocoll* . **2023** , *142* , 108798. https://doi.org/10.1016/j.foodhyd.2023.108798

**Tables**

**Table 1.** Specific activity of*Pd* PDH[a] and mutants toward galactitol using either $NAD^+$ or $NADP^+$.

| Enzyme | Specific activity (U $mg^{-1}$) [b] | Specific activity (U $mg^{-1}$) [b] |
|---|---|---|
| | $NAD^+$ | $NADP^+$ |
| WT | 25.42 ± 1.37 | n.a.[c] |
| D36A | 20.31 ± 0.85 | n.a. |
| D36G | 24.46 ± 0.65 | n.a. |
| I37R | 22.03 ± 0.86 | n.a. |
| D36A/I37R | n.a. | 19.40 ± 0.99 |
| D36G/I37R | n.a. | 18.23 ± 0.95 |
| D36R/I37R | n.a. | 11.36 ± 0.30 |
| D36H/I37R | n.a. | 18.02 ± 1.30 |
| D36K/I37R | n.a. | 17.58 ± 0.52 |
| D36I/I37R | n.a. | 6.62 ± 1.26 |
| D36F/I37R | n.a. | 12.36 ± 0.26 |
| A14T | 13.55 ± 0.75 | n.a. |
| A14S | 13.58 ± 0.74 | n.a. |
| A14T/D36A/I37R | n.a. | 18.02 ± 0.34 |
| A14S/D36A/I37R | n.a. | 17.65 ± 0.07 |

[a] *Pd* PDH, polyol dehydrogenase from*Paracoccus denitrificans* ; [b] One unit is defined as the amount of protein that produces or consumes 1 µM of NAD(H)/NADP(H) per second; [c] n.a. = no measurable activity.

**Table 2.** Kinetic parameters of *Pd* PDH mutants determined with $NAD^+$ or $NADP^+$ using galactitol as substrate in excess.

| Enzyme[a] | $K_m$ (mM) | $K_m$ (mM) | $k_{cat}$ ($s^{-1}$) | $k_{cat}$ ($s^{-1}$) | $k_{cat}/K_m$ ($mM^{-1}$ $s^{-1}$) | $k_{cat}/K_m$ ($mM^{-1}$ $s^{-1}$) | Vmax (µm |
|---|---|---|---|---|---|---|---|
| | $NAD^+$ | $NADP^+$ | $NAD^+$ | $NADP^+$ | $NAD^+$ | $NADP^+$ | $NAD^+$ |
| WT | 0.7723 | i.g.[b] | 0.3763 | n.a.[c] | 0.4872 | n.a. | 1.028 |
| D36A/I37R | i.g. | 0.942 | n.a. | 0.3040 | n.a. | 0.3224 | n.a. |
| D36G/I37R | i.g. | 1.299 | n.a. | 0.2831 | n.a. | 0.2179 | n.a. |
| D36H/I37R | i.g. | 1.305 | n.a. | 0.2673 | n.a. | 0.2048 | n.a. |
| D36K/I37R | i.g. | 1.355 | n.a. | 0.1103 | n.a. | 0.0814 | n.a. |
| D36I/I37R | i.g. | 1.801 | n.a. | 0.1411 | n.a. | 0.0783 | n.a. |
| D36F/I37R | i.g. | 1.378 | n.a. | 0.0776 | n.a. | 0.0563 | n.a. |
| D36R/I37R | i.g. | 1.603 | n.a. | 0.0673 | n.a. | 0.0420 | n.a. |
| A14T/D36A/I37R | i.g. | 1.259 | n.a. | 0.1084 | n.a. | 0.0861 | n.a. |
| A14S/D36A/I37R | i.g. | 1.308 | n.a. | 0.1071 | n.a. | 0.0819 | n.a. |

[a] All enzymes were purified before characterization. For determining kinetic parameters, the initial rate of the enzyme was measured in 100 mM Tris-HCl pH 8.0 with $NAD^+$ or $NADP^+$ (0.2 mM) in the presence of saturating concentrations of substrate galactitol (50 mM) at 30 °C; [b] i.g. = infinitely great;[c] n.a. = no measurable activity.

**Table 3.** Information on the pathway conditions.

| | Pathway I | Pathway I | Pathway I | Pathway II | Pathway II | Pathway II | Pathway II | Pathway II | Pa II |
|---|---|---|---|---|---|---|---|---|---|
| | Condition 1 | Condition 2 | Condition 1 | Condition 1 | Condition 2 | Condition 3 | Condition 4 | Condition 5 | Co 6 |
| *Ps*XR (mM) | 18 | 18 | 18 | 18 | 18 | –[a] | – | – | – |
| *Pd*PDH (mM) | 36 | 36 | – | – | – | – | – | – | – |
| *Pd*PDH$^{D36A/I37R}$ (mM) | – | – | 36 | 36 | 18 | – | – | – | – |
| *Ps*XR-Linker-*Pd*PDH$^{D36A/I37R}$ (mM) | – | – | – | – | – | 18 | – | – | – |
| N[b]-SpyTag003-*Pd*PDH$^{D36A/I37R}$ (mM) | – | – | – | – | – | – | 18 | – | 18 |
| C-SpyTag003-*Pd*PDH$^{D36A/I37R}$ (mM) | – | – | – | – | – | – | – | 18 | – |
| N-SpyCatcher003-*Ps*XR (mM) | – | – | – | – | – | – | 18 | 18 | – |
| N-SpyTag003-*Ps*XR (mM) | – | – | – | – | – | – | – | – | 18 |
| EutM-C-SpyCatcher003 (mM) | – | – | – | – | – | – | – | – | 36 |
| lactose (mM) | 20 | 20 | 20 | 20 | 20 | 20 | 20 | 20 | 20 |
| NADPH (mM) | 2 | 1 | 2 | 2 | 2 | 2 | 2 | 2 | 2 |
| $NAD^+$ (mM) | – | 1 | – | – | – | – | – | – | – |

[a] Dash indicates no addition;[b] N or C means that SpyTag003 or SpyCatcher003 fused to an N-terminus or C-terminus of *Ps* XR or*Pd* PDH$^{D36A/I37R}$.

**Table 4.** D-tagatose production with lactose and whey powder.

| Materials | D-tagatose concentration (g/L) | D-tagatose yield (g/g lactose) | D-tagatose yield (g/g whey powder) | C |
|---|---|---|---|---|
| Lactose [a] | 35.7 | 0.357 | - | 0 |
| Whey powder [b] | 32.9 | 0.329 | 0.269 | 0 |

[a] 100g/L lactose in the solution.[b] 100g/L lactose in cheese whey powder.

**Figures and legends**

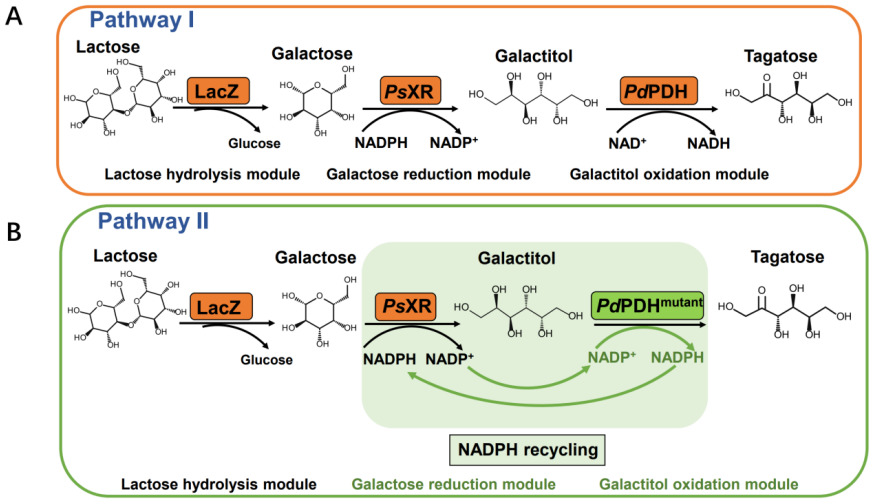


**Figure 1.** Schematic diagram of the production of tagatose from lactose via the oxidoreductive pathways. A: Pathway I without cofactor cycle; B: Pathway II with NADPH cycle.

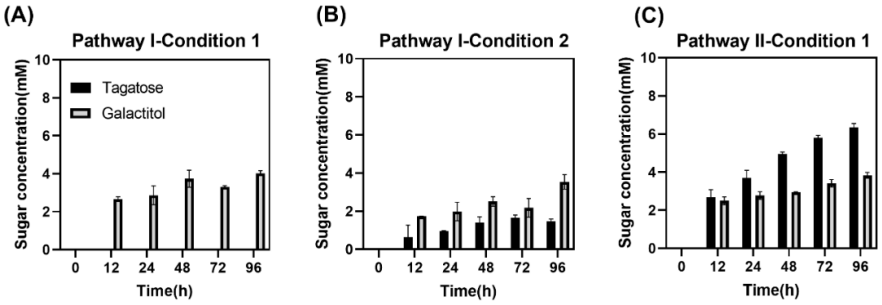


**Figure 2.** Validation of D-tagatose synthetic pathways. All reactions were performed with 20 mM lactose, 100 mM Tris-HCl (pH 8.0) at 30 °C. The information on pathway conditions is shown in Table 3. The yields of tagatose and galactitol in (A) Pathway I–Condition 1, (B) Pathway I–Condition 2, and (C) Pathway II–Condition 1 are shown. Experiments were performed in triplicates, and error bars represent the standard deviation.

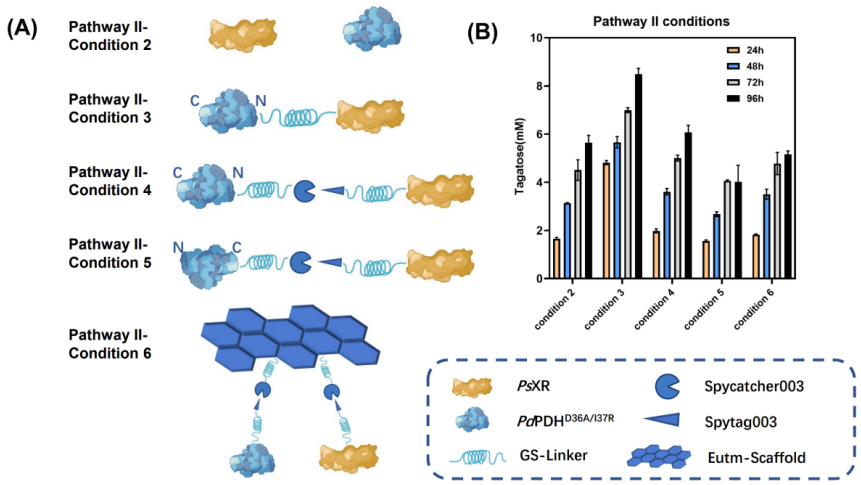


**Figure 3.** D-tagatose yield with different enzyme cascade strategies.

(A) Schematic diagram of different enzyme cascade strategies. (B) D-tagatose yields at 24, 48, 72, and 96 h of reaction in 100 mM Tris-HCl (pH 8.0) at 30 °C. Markers correspond to those in Figure 3A. The information on pathway conditions is shown in Table 3. Experiments were performed in triplicates, and error bars represent the standard deviation.

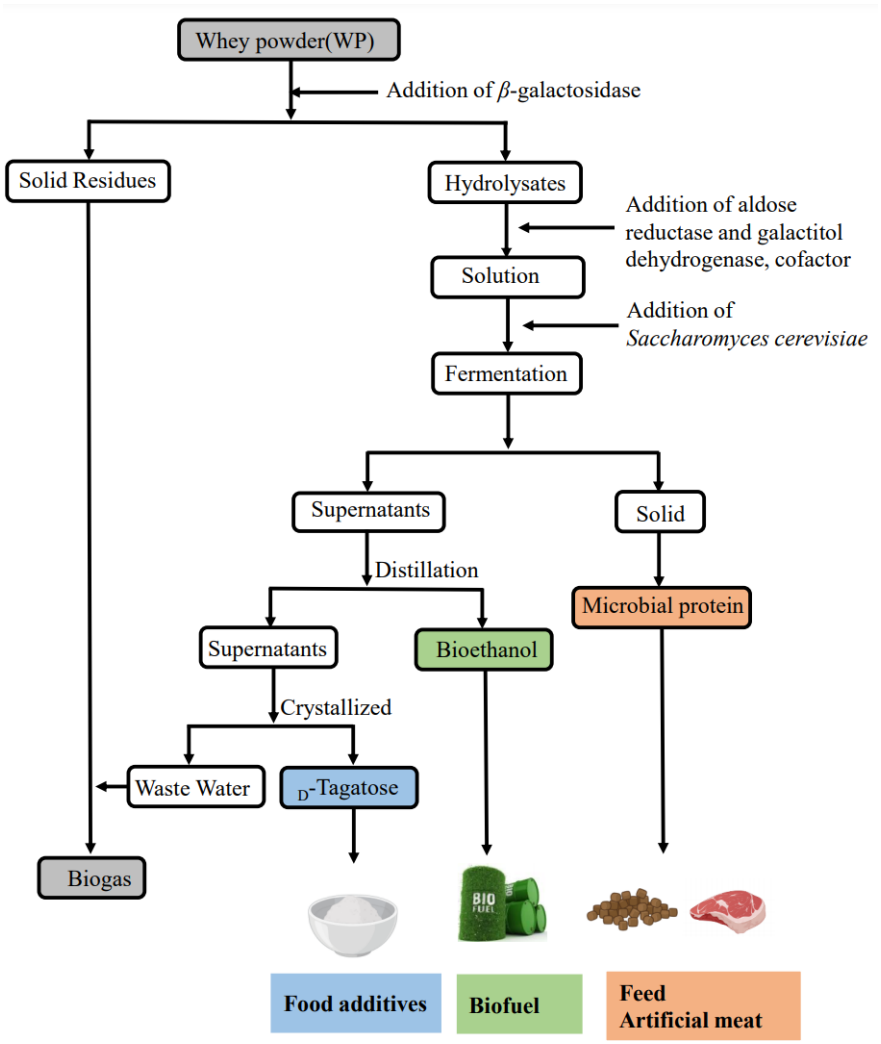


**Figure 4** . A scheme of the overall process for coproduction of$_{D}$-tagatose, bioethanol, and microbial protein from whey powder.

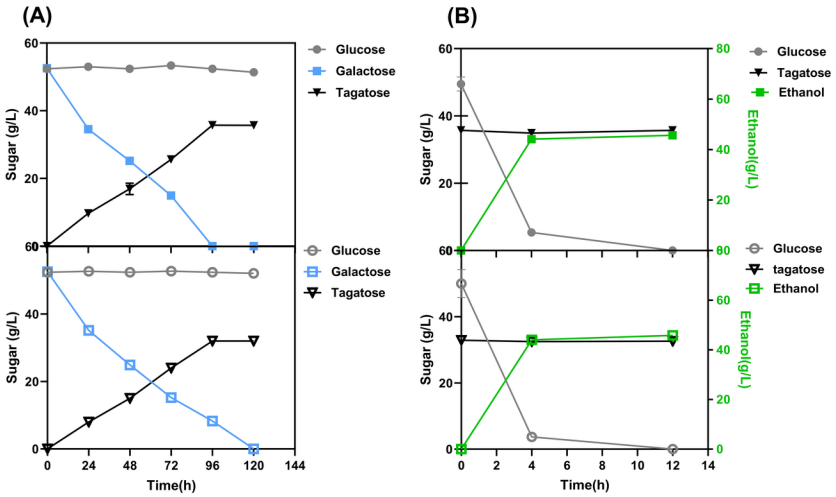


**Figure 5** . Time course of D-tagatose production from 100 g/L lactose and 122 g/L cheese whey powder (including 100 g/L lactose) (A). Fermentation of mixed sugar syrup derived from lactose and cheese whey powder by *S. cerevisiae* (B). Solid dots represent lactose as substrate, and hollow dots represent whey powder as substrate. Experiments were performed in triplicates, and error bars represent the standard deviation.

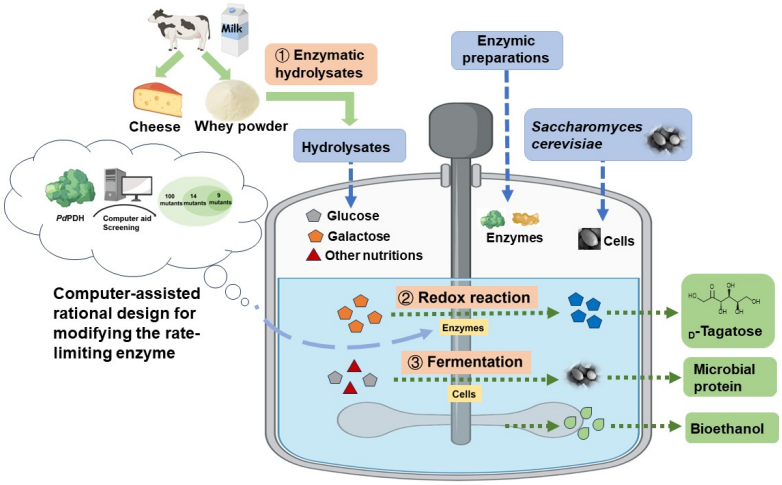


**Synopsis:**

One-pot integrated bioprocess for the coproduction of D-tagatose, bioethanol, and microbial protein from whey powder.